EEG/EMG Using Dry Electrodes

Nick Arango

5/14/2015

1 Introduction

This paper presents a EEG/EMG measurement device designed for applications in computer interface and sleep monitoring. This device attaches to the users scalp and face using dry, bed of blunt needle, probes which is more convenient for users and posed interesting design challenges. The final device was able to recognize blinking of a user's eyes through EMG signals, provide data to a computer about the direction of a user's eyes through EMG signals, and measure EEG signals to some degree. Testing was a challenge due to the small voltage levels of EEG and EMG signals. Using the device to measure Electrocardiograms (ECGs) proved to be a simple way of validating correct operation before measuring the smaller EEG and EMG signals.

1.1 Motivation

Measurement of microvolt scale signals on the skull correlated with brain activity can provide useful data for doctors diagnosing sleep or brain disorders. Similar signals generated by the motion of the eyes is similarly useful. The cost of electroencephalograms (EEGs) used to measure brainwaves and electromyograms (EMGs) have decreased dramatically and consumer products promising in home sleep monitoring. Even simple mind control toys have come to market.

These products amplify the small EEG/EMG signals, digitize these signals, and perform simple digital filtering to extract signals correlated with different thought patterns, sleep cycles, eye movement or blinking.

The signal processing needed to analyze sleep, concentration or eye movements is relatively simple. In the case of EEG, the measured signal is split into several frequency ranges each correlated with different brain activity. The relative magnitudes of the frequency ranges indicate the type of brain activity. Due to the low frequency of the signals involved these signals can be computed by low power microcontrollers or analog electronics.

There are two standard ways of electrically connecting EEG/EMG circuitry to a user's head that each provide different strengths. Passive wet electrodes use a conductive gel to provide an electrical connection to a user. These electrodes can not contact skin through hair and are either non-reusable or require cleaning after each use. They do provide an advantage of low output impedance reducing noise in the system. Dry active electrodes can make contact through hair and don't require cleaning. However, their output resistance

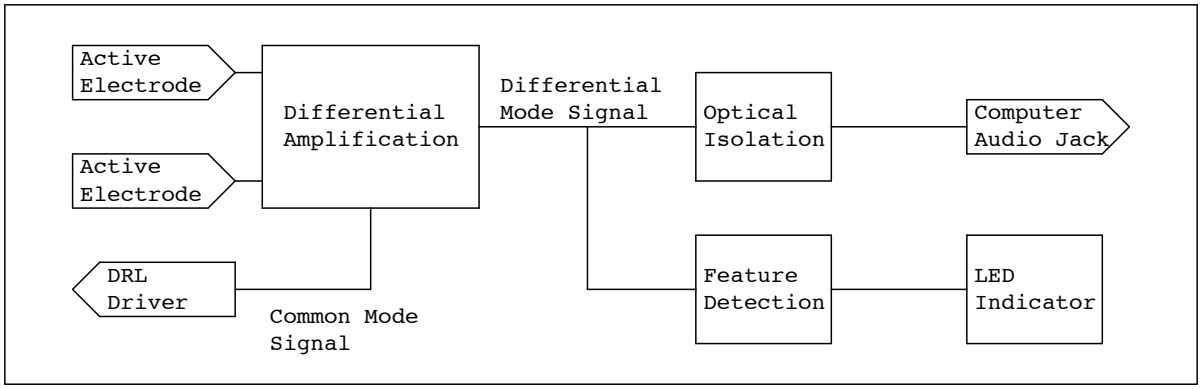

Figure 1: High level block diagram of the portable low noise EEG/EMG. Active electrodes connect to the scalp and face of the user and the output attaches the the laptop of the user. An LED indicates when the user blinks.

is rather high and need additional circuitry to reduce noise. In consumer applications dry active electrodes are their obvious choice due to the lower maintenance at the cost of increased circuit complexity.

1.2 Changing Scope and Goals

This project initially aimed to create a portable electroencephalogram (EEG) for use as a computer interface device with low setup and cleanup time. To achieve this goal we built active dry electrodes, filtered differential amplification, analog optical isolation and analysis circuitry. As the device was tested it became clear that EEG data was not sufficiently reliable both due to the circuit and due to the nature of EEG so EMG signals of the eye became the demoing benchmark. These signals were still on the order of 50uV so the design of the amplifier was similarly challenging, just simpler to test.

2 Design

2.1 System Overview

The body potential measurement device, at a high level, has four major components: dry active probes, low-noise high-gain differential amplification, analog signal processing, and analog optical isolation. A system diagram is shown in figure 1.

The dry electrodes connect to the circuit to the user and require active buffering or amplification to drive the long signal wires with a low output impedance. The low impedance reduces electromagnetic interference.

The differential amplifier end takes small signals from dry electrodes attached to the scalp and amplifies the microvolt level signals at the frequencies 1 and 40 Hz that are correlated with brain activity and muscle contraction. Because the sensed signals are so small, immunity from outside noise sources and reduction of noise from electrical components

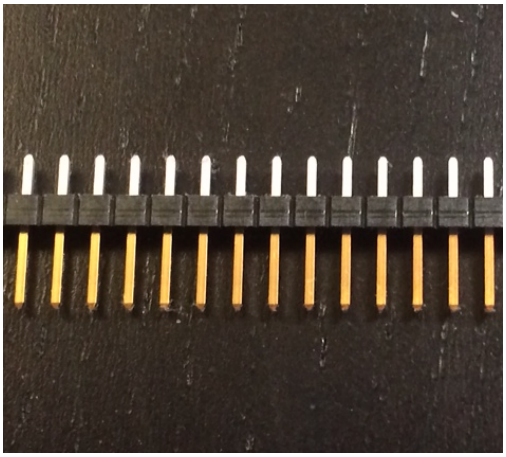

Figure 2: Headers used in the dry electrode

is critical. Fortunately the main component of interference, 60 Hz mains hum, is outside of the relevant frequency range for EEG and EMG and therefore is filtered out. The other major sources of noise are ripple on the power supply, RF interference on high impedance signals and component drift.

Because the EEG signal is inherently differential, once buffered, the electrode signals will be subtracted in a differential amplification stage. The common mode signals will provide an additional noise source and while this is mitigated by the common mode rejection ratio of the amplifiers, further action can be taken. To reduce this source of noise, the body is driven to a potential to cancel out the common mode voltage of the electrodes. The common mode signal was be low passed before driving the body to prevent instability.

The design of this circuit posed challenging due to the low noise requirements. Testing also presented a set of challenges. Bench function generators don't provide the microvolt level signals needed to test the electrode buffers and differential amplifier. However, simple resistor attenuators can provide the necessary signals at reasonable common modes. Each of the amplifiers were tested individually prior to integration in the front end by measuring the frequency response given microvolt inputs.

2.2 Characterization of Dry Electrode

Characterization of the connection between the dry electrodes and a user's skin was important in designing the low noise active probe amplifiers. An LRC meter was used to measure the contact resistance of the needle electrodes over a range of frequencies. For a baseline, wet electrodes were attached to the forearm 6 inches apart and the LRC meter was used to measure the sum of the two contact resistances plus the resistance of the skin. One of the wet electrodes was removed and replaced with a dry electrode and the experiment was run again. The readings were compared to determine how much worse the dry electrodes were as compared to the wet electrodes. Table 1 summarizes these results. Frequencies between 5 and 100 Hz were tested. The lower limit was a limitation of the LRC meter and all relevant measured signals would be well below the upper tested limit. Note that the resistance of human skin at a distance of 6 inches is on the order of kilaohms.

Frequency (Hz)	5	7.5	10	15	25	35	45	55	65	75	85	95	100
Wet Resistance (MOhm)	.24	.16	.13	.12	.09	.07	.05	.05	.04	.04	.04	.04	.03
Dry Resistance (MOhm)	.52	.45	.43	.41	.39	.39	.39	.37	.37	.37	.37	.36	.36

Table 1: Wet and dry electrode resistance resistance as a fucntion of frequency

The contact resistance of the dry electrode was not just a function of frequency but also a hysteretic function of pressure. If the needles very lightly touched skin, a reading of 10's of mega Ohms was measured. There was some critical pressure after which the resistance was characterized by the transfer data in table 1. If the probes was removed and replaced or translated the resistance would increase to 10's of mega Ohms again.

This is most likely due to the pressure of the electrodes on the skin piercing through the Stratum Corneum composed of dead skin and touching the living Stratum Spinosum, a more conductive, living layer of skin cells. This gave insight on how to place electrodes on a users body for both comfort (minimizing pressure) and optimal sensing (minimizing contact resistance).

2.3 Active Probes

The design of the active probe circuit depended on the electrical characteristics of the dry electrodes. Because of the high source impedance of the electrodes, the amplification circuit had to be physically very close to the electrode. By minimizing the length of wire between the electrode and the amplifier, common mode interference was reduced. The physical proximity suggested that the circuit needed to be small and therefore simple. To prevent interference on long power supply wires each amplifier was powered by a small battery necessitating the use of low power components. Additionally, the high gain in subsequent stages of the circuit required a low output bias from the active probes. Bias of less than a millivolt was necessary to prevent clipping in further stages. A simple non-inverting amplifier was implemented and though the circuit is simple, great care was taken in the selection of the amplifier to meet the specification. A schematic of the active probe is shown in figure 3a. The gain of two was selected to ensure the correct operation of subsequent stages of the circuit. With too much gain, the DC bias becomes unmanageable for future stages. The feedback capacitor was added to reduce high frequency gain to unity. Because the input stage was noninverting, reducing high frequencies below unity gain was not possible while maintaining high input impedance. The pin labeled S is an active low shutdown pin with an internal pullup to turn off the amplifier and reduce power. In this application this pin was left floating. The two dominant sources of noise from the circuit itself are input offset voltage noise and input offset current noise. The power spectral density (PSD) of both of these noise sources behave like a single pole at zero and a zero at some higher frequency. The frequency range relevant of the input signals of this circuit ends well before the zero in the noise PSD and therefore must contend with the large low frequency noise refered to as 1/f noise. In selecting an opamp for this application, first input offset voltage and input offset current were considered. Only JFET or CMOS input stage amplifiers were considered due to their high input impedance and any amplifier with an offset voltage greater than 500mV was rejected. This rejected the jellybean LM356 JFET input opamp with its 5mV offset. While this component has

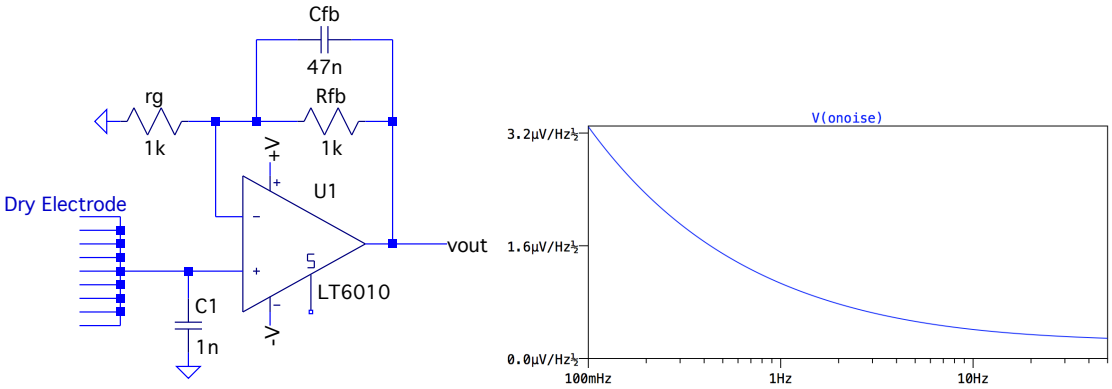

(a) Active probe schematic (b) Input referenced noise spectral density

Figure 3: The active probe was designed to maximize input impedance, minimize output offset voltage, and minimize noise.

external trimming capability, re-tuning a potentiometer josteled through use did not seem like a viable option. Then the input offset voltage and current specifications were considered. Because the source impedance was on the order of 300kOhms (as determined in the previous section) current mode noise could be ignored if RMS current noise $\times$ 300kOhms is very much less than the voltage mode noise. Unfortunately this was not the case for any of the practical opamps. After LTSpice noise simulation of many amplifiers, the LT6010 was selected even though its RMS current noise was larger than other components. If the source resistance of the electrode was twice as large the LT6014 would have been selected as it has higher voltage noise but lower current noise. A PSD of the amplifier noise is shown if figure 3b. The RMS noise between the frequency of .1Hz and 50Hz is 3.1μVolts

The noise performance and fidelity of the LM6010 was verified by configuring the opamp as a non inverting amplifier with a gain of 1000 and driving it with 10uV 1kHz sine wave generated by dividing a 10mV sine wave with a voltage divider in addition to measuring its zero input response. The low frequency noise was very visible in slow shifts of the offset of the 1kHz output. The RMS of this noise was estimated at 2mV RMS between 0Hz and 50Hz referenced to the output and therefore 2μVolts referenced to the input, validating the specification of the device.

This component has advantages in power consumption. During normal operating conditions, simulation suggests a power consumption on the order of 70μ watts. This is result is backed up by imperial observation. The active probes were constructed on two small breadboards individually powered by nine volt batteries. A picture is shown in figure **??** These were left on continuously for the two weeks after their construction and the voltage of the batteries fell by less than 5mV in that time. Theoretically, one 9V battery could power an active probe for 8.7 years, well longer than the shelf life of the battery.

The image shown has one component missing: the audio jack that connects the active probe to the subsequent stages. An audio jack was a convenient cable because of its flexibility, plug ability, and they have three conductors. One conductor was used as ground, another was for virtual ground, and the third for signal. The other end of the audio cable connected to the subsequent differential amplification stage.

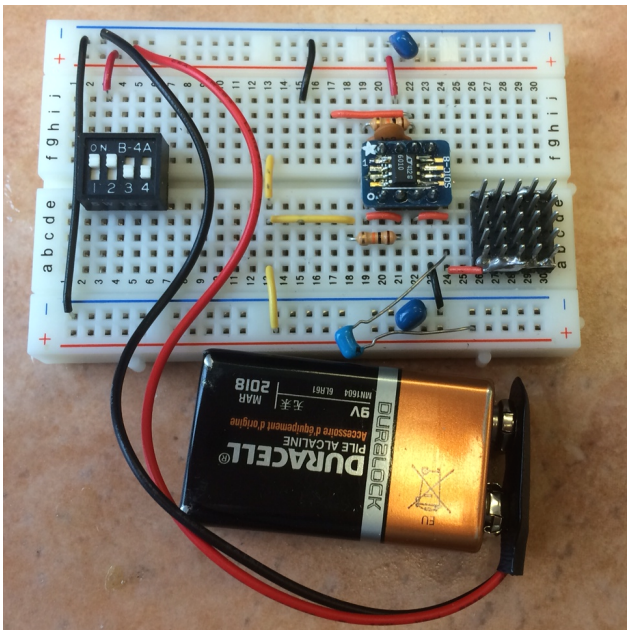

Figure 4: Image of one active probe showing the dry electrode, LM6010, and 9 volt power source

The image also shows significant room for improvement in the layout of the active probe to buffet noise immunity. A short orange wire soldered directly to the solder bridge that connects the pins connects the LT6010 through a breadboard row to the probe. Neither the needles nor the high source impedance wires connected to the needles are shielded. If this circuit were laid out on a PCB, a virtual ground plane would shield

2.4 Differential Amplification

Differential amplification is accomplished with an instrumentation amplifier and circuitry to reject noise and DC offset. The common mode signal is also calculated by the circuit. This subsystem, in addition to all subsequent subsystems, is powered from a third nine volt battery. A virtual ground is generated using a rail splitting voltage divider and a non-inverting buffer. A complete schematic is show in in figure 5

The AD610 instrumentation amplifier was used to subtract the signal from the two probes. Its 120dB common mode rejection ratio, high power supply rejection ratio, and low input offset voltage make it an ideal part for this application. The 50uV input offset voltage permits the use of large gains. A gain of approximately 50 was used in this application and was set with a 1kOhm gain resistor. This was implemented with two series 510 ohm resistors which allowed for the measurement of the common mode signal. To prevent loading on that gain resistor center tap, the common mode signal was buffered with a rail to rail opamp. Rail to rail operation is important here because the common mode signal may vary widely and this signal is used in the right leg drive circuit to compensate for common mode offset.

Two Sallen Key lowpass filters both with a gain of 10 amplify the differential signal while

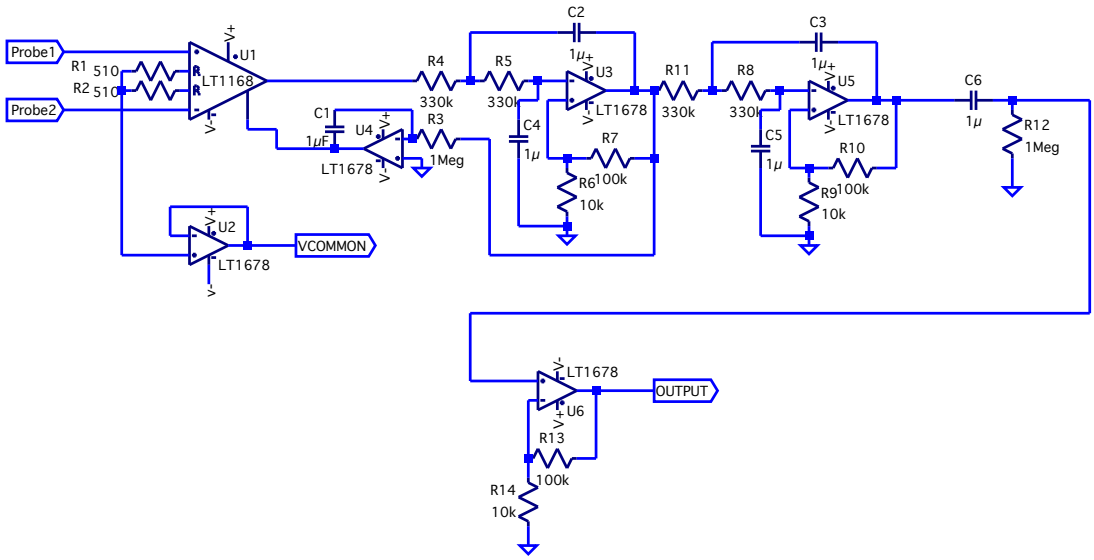

Figure 5: Schematic of the differential amplification stage. U1 is an instrumentation amplifier to measure the differential mode of the probe signals. U2 buffers the common mode voltage. U3 and U5 provide filtering to reject mains and RF interference. U6 is an additional gain stage. U4 uses feedback to reduce the DC component of the system

attenuating frequencies above 50Hz. The cutoff frequency was chosen to allow as much signal through as possible while being far enough away from 60Hz to attenuate the large mains interference. At the output of U1 the signal is 250mV peak to peak but it is mostly 60Hz noise. The filtering stages allow for the amplification of the signal within the noise without causing clipping. Four poles were necessary to limit the 60Hz interference to less than one percent of the signal because the cutoff frequency is so close to the major source of interference.

With all of the amplification the differential signal, DC biases and input offset voltages are magnified. Feedback from after the first Sallen Key filter drives the instrumentation amplifier's output bias point pin. The signal is integrated to prevent steady state error in the DC bias. The resistor and capacitor for this filter were sized to provide sufficient gain to correct DC bias errors on the order of a second. The DC bias is taken from the first Sallen Key filter because feedback taken from later in the system caused ringing caused by reduced phase margin near 60Hz and occasional clipping of the intermediate stages. Instability would not have been a problem if these stages had less gain, but because of the gain, phase approached 180 well before 0dB.

Feedback couldn't be used to remove the DC offset from the output of the second Sallen Key filter so before further amplification, the signal passes through a passive highpass filter.

Even when properly compensated for, input DC bias can still cause problems. Because the gain stage of the instrumentation amplifier is not effected by the output bias adjustment, signals with a large differential mode DC bias can clip and loose information before their bias is removed by the differential stage of the instrumentation amplifier. Fortunately, the DC bias found between electrodes in the full system was less than the 180 mV that caused clipping.

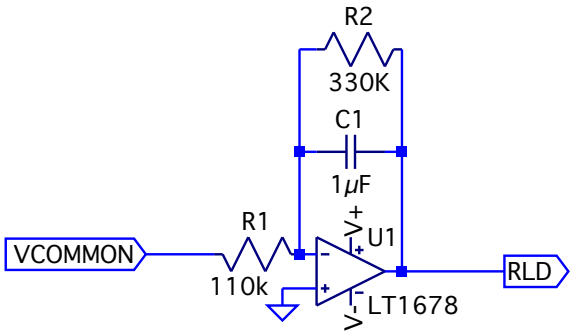

Figure 6: Schematic of the right leg driver circuit

2.5 Right Leg Drive

The right leg drive (RLD) circuit set the user's common mode voltage to increase the effective common mode rejection ratio of the circuit. The name right leg drive is a holdover from ECG technology where the right leg is driven to a known potential to avoid interfering with the operation of the heart. In this application the right leg drive was connected to the center of a user's forehead using a wet adhesive electrode.

The RLD circuit simply low-passes the common mode voltage measured by the differential amplification stage. This amplification stage had a gain of 3 and a frequency cutoff of approximately half a hertz. The system was tested with higher gains and lower cutoff frequencies to improve the common mode rejection ratio but this lead to instability. Ideally, the passband of the RLD circuit would include 60Hz to reject the main source of common mode noise. Unfortunately the reactance of the body at that frequency caused phase shifts and significantly reduced open loop phase margin resulting in oscillation. A cleverer analysis of skin impedance might have provided insight into the construction of a lead network to compensate for the user's skin to provide more gain at 60Hz. Time constraints did not permit that rigor of analysis.

The DRL was set to a higher voltage than the common mode measured by the instrumentation amplifier. This was most likely due to the increased resistance of the wet adhesive probe at DC. In an attempt to avoid steady state error, the circuit was modified to act as an integrator by removing the feedback resistor and increasing the input resistor. The use of an integrator as a DRL output drove the system unstable. The exact mechanism for the instability is not understood.

2.6 Feature Detection

When the active probes are connected the the user to measure EMG signals, eyes movements and blinks are easily observable in the EMG signal on the oscilloscope. For example electrode placement was configured measure blinks, a 200mV 4ms pulse with a sharp leading edge and a gradual lagging edge is apparent on the EMG signal. Where the electrodes were placed to acheive this measurement is described in section 2.8

While the previous stage performed well in blocking the DC component of the signal

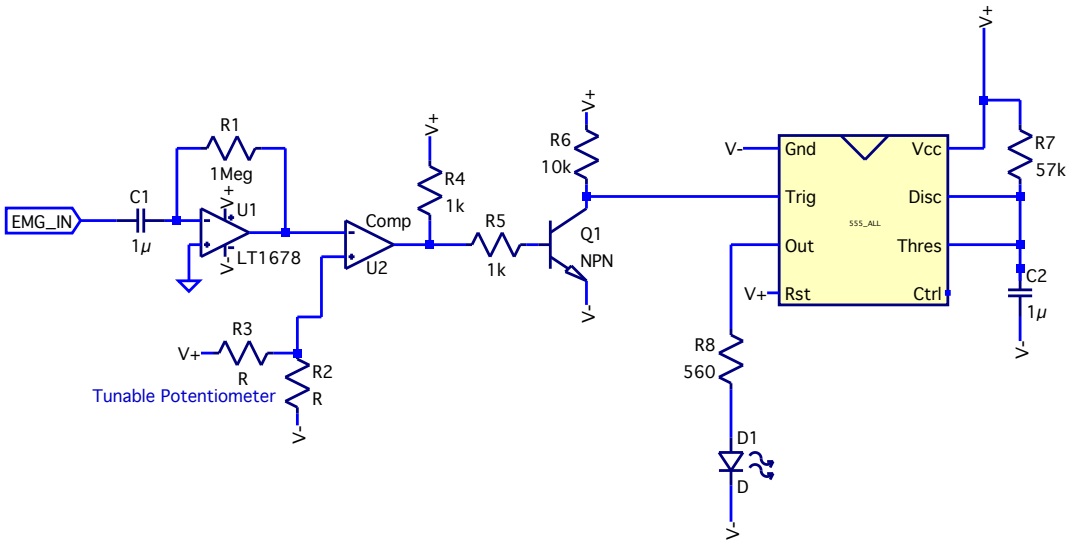

Figure 7: Schematic of the blink detection circuit. A differentator generates a pulse on the edges of blinks and a comparator thresholds that signal to generate a pulse on blinks. A 2n3904 is used as an inverter to generate an active low trigger signal for the 555 timer which flashes the LED for a visible duration for each blink.

associated with the positioning of the electrodes, small variations in the pressure of the electrodes on a user's skin caused small, temporary changes in the DC offset of the EMG signal. The noise associated with electrode pressure could not entirely filtered out because it occurs in the frequency range of interest. Thresholding the EMG signal directly to detect blinks caused spurious readings due to the wandering offset whenever the user moved the probes. Because of the sharp rising edge of the signal, the derivative of the EMG reading provided a clean way to detect blinks.

This signal was thresholded using the LM1011 comparator. The duration of the compared signal is was short and while it was visible on the oscilloscope, that did not provide a compelling demonstration. A 555 timer was configured as a monostable oscillator to pulse and drive an LED whenever the user blinked. The compared signal was inverted with a common emitter amplifier to generate the active low trigger for the timer IC.

Setting the threshold of the comparator required some skill. Two hands were needed to hold the electrodes to the users face and a third was needed to adjust the potetiometer setting the reference voltage. Imaginably, this was quite tricky for a single person to manage. Ideally this threshold could have instead been calibrated dynamically by estimating the peak to peak voltage when the user was not blinking, adding cushion room and storing that voltage in a sample and hold. Unfortunately, there was not enough time to complete the construction of that circuit.

2.7 Analog Isolation

Optical isolation between the EEG/EMG and a recording device allows enables the use of mains powered recording equipment without sacrificing signal quality. Referencing the high

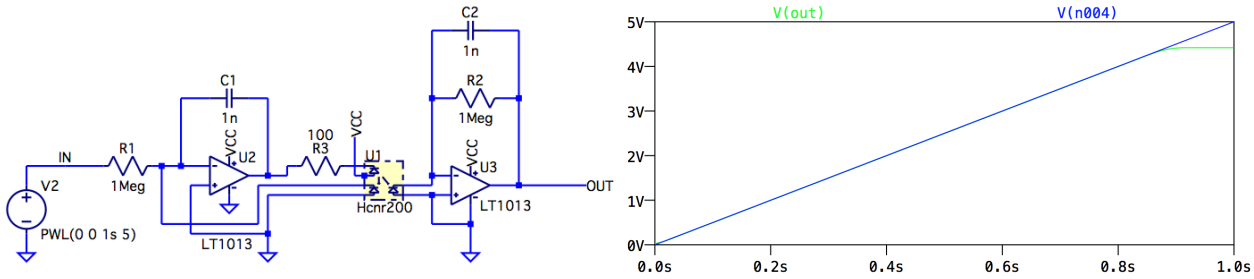

(a) Isolation schematic.

(b) Voltage transfer function

Figure 8: The analog optoisolation circuit provides 5kV voltage isolation between the EEG/EMG and the recording device while providing high lineary through much of the power supply range. THe green trace shows the output where the blue trace shows the input

gain amplifiers to earth ground can introduce large common mode voltages (at DC and at 60Hz) to the input of the differential amplifier. To reduce the effect of this noise, the EEG/EMG circuit is battery powered and electrically isolated from wall.

Most isolation techniques are aimed at digital signals. The usual approach for passing an analog signal across an isolation barrier is to first digitize it with with an analog to digital converter and then pass the signal over the isolation barrier either galvanically or optically. Both optical isolators and non integrated galvanic isolators have poor linearity to isolate an analog signal without resorting to digital techniques feedback was necessary. A circuit to galvanically isolate analog signals is similar to an isolating DC/DC regulator with the output voltage set equal to the input signal. Integrated solutions exist but a discrete design would be large, complicated, and introduce high frequency power supply ripple. Optical isolation Figure **??** shows the schematic of the circuit that enables the isolation.

This circuit uses the HCNR200 linear analog optocoupler from Avago Technologies that contains a single LED and a pair of photodiodes with matched optical characteristics. One photodiode lies on the driving side of the isolation barrier and the other lies on the receiving side. Transimpedance feedback is used to to set the current through the drive side photodiode and because the two diodes are matched, also the current in the receive side diode. By sensing the current through the receive photodiode with a transimpedance amplifier with the same feedback resistor as the drive side, the output voltage is equal to the input voltage. The feedback resistor is selected to provide sufficient gain to overcome the nonlinearities of LED-photodiode system. One Mega Ohm was sufficient to provide a high degree of linearity. The LED drive resistor is selected to prevent over-current if the full power supply were applied over the LED and resistor in series. The one nanofarad capacitors reduce high frequency gain to maintain stability. The LED-photodiode system acts as a lag network so the system would be unstable without this compensation.

Deviation from of the output from the input in the spice simulation in figure 8b is due to the limitations of the opamps. If the opamps operated rail to rail, the region of linearity would continue further.

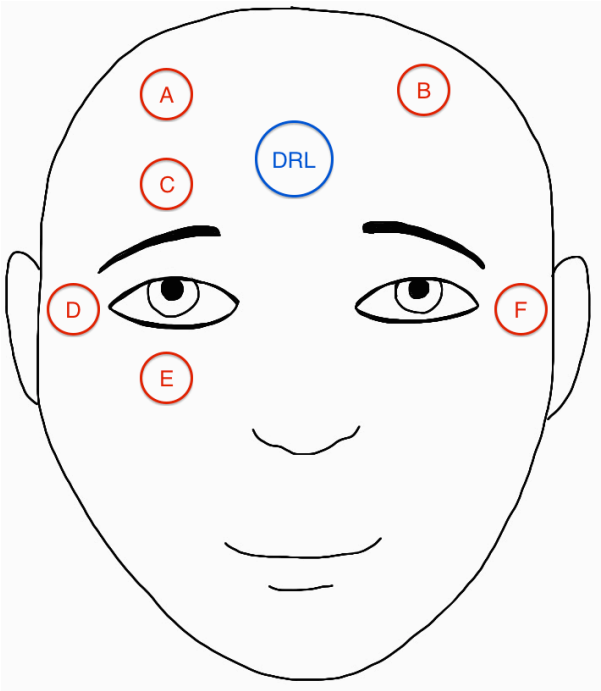

Figure 9: Placement of electrodes to make different measurements. A-B provides EEG. C-E measures blinking and virtical eye movement. D-F measures left-right eye movement. Driven right leg(DRL) is driven from the circuit sets the common mode voltage

2.8 Electrode Placement

Electrodes could be placed in various positions on the face and scalp to measure different body potentials. Figure **??** shows a face and the positions of electrodes to measure different features. The designed in this paper was able to conclusively measure blinks with electrodes placed on top an bottom of one eye and the motion of the eye to the left and right when the electrodes were placed at the temples. The DRL was adhered to the center of the forehead to minimize the DC bias between two electrodes.

Through experiments conducted with three wet electrodes on the forearm, electrodes spaced at unequal distances from the driving electrode measure different common mode voltages. This was initially attributed to the resistance of the body but the LT6010 amplifiers have such low input current that this explanation seemed unreasonable. The exact mechanism is not known but through experimentation, increased symmetry in the placement of the electrodes resulted in reduced differential mode DC offset. The placement of the DRL electrode also effected the influence of common mode noise. The further the electrode was placed from the measurement site, the larger the 60Hz common mode interference. This is likely due to the resistance of skin.

When testing the device it was important to understand that the measured signals were coming from body voltages rather than the jostling of the electrodes on the skin resulting in

changes in the DC bias of the differential mode signal. To verify that the measurements were, in fact, what we intended to measure, electrodes were pressed against the face and moved around without blinking or moving the eyes. A very large translation or change in pressure was needed to generate voltages comparable to that of a blink signal. It was concluded that the measurements on all of locations shown in figure **??** were not spurious or due to the slight movements of skin.

3 Performance

3.1 Noise

In the design of the active probes, component noise was taken as a dominant source of error and the system was designed around minimizing this error. Because of the high source impedance of the electrode electromagnetic interference played a major role. While most of this noise was well above the 40Hz maximum frequency of interest of EEG signals, preventing this interference from overpowering our signal was a large point of effort in this project. Before the low frequency component noise was a factor the 50uV-100uV input differential signal was swamped by 60Hz and high frequency noise on the order of 10-100mV. Instead of focusing so much on the 1/f noise from opamps, the practical consideration of radio interference should have been dealt with first. Shielded cabling and a well designed pcb for the electrodes would have gone far in this department. None the less the 3uV RMS low frequency input referenced noise was visible on the output after sufficient low-pass filtering. Component noise was small enough such that it only effected signal quality not the topology of the circuit to prevent clipping.

When a nearby group operated their FM radio (outputting approximately 1.5 watts), the signal measured from the probes was completely overwhelmed. The sum of two FM waves of slightly different fundamental frequencies was visible on on the output of the as an AM envelope of the beat frequency. This was measured directly on the probe breadboard and was not a result of coupling through the long audio cable. Instead this signal had to couple directly into the electrode pins. This was only an issue when this transmitter was physically near the EEG/EMG and transmitting at full power. This example of radio interference prompted a more careful analysis of the clipping levels of each stage.

While interference on the electrodes was mitigated by the design of the circuit, the electrodes still had to be used properly to measure the desired signals.

3.2 Repeatability and Usability

Proper electrode placement was key to the correct operation of the circuit. When I placed electrodes on the facial skin to measure EMG, watching an oscilloscope trace of intermediate signals in the circuit helped give feedback for adjusting placement and pressure. With inadequate pressure, no signal was measured, and with too much pressure even the dull needles started hurting the user. Too much pressure also caused an increase in noise. Ideally an additional circuit could be designed to guide the user with LEDs for feedback rather than an oscilloscope.

Because feedback was critical to the placement of the electrodes, measurements of EEG signals were very difficult to 'lock on' to. I had no way of knowing if the circuit was operating properly and the electrodes were incorrectly placed or the electrodes were off and the circuit was working correctly. As a result, EEG signals were confidently measured only once after several hours of fiddling.

The system would have been much more usable with a headband to connect the probes to the user. Unfortunately, when this was attempted, the needle like electrodes caused pain in the user's face.

3.3 Notes on Testing

Testing of individual components in this system relatively simple, but integration testing required a human subject. For example, the RLD operation was verified by adjusting the common mode of the signal input into the system from the function generator, but to understand the potential instability of the feedback system the RLD had to be connected to a user. As a result, the only way to fully test this part of the system was by integrating it into the full system including the user. A project measuring body potentials like this was full of many hours with electrodes pressed to my face and trying to see the oscilloscope to understand the state of operation at the time.

4 Extensions

Potential for further work on this project has been described throughout the document but these improvements fall into three major categories.

1. Improved modeling

   More accurate models of the body system that the EEG/EMG device connects to would enable the construction of better test circuits. Instead of testing the integrated design on human subjects that give little insight as to where errors occur, better modeling would bolster repeatable tests. More accurate models would also give an indication of the causes of several instability problems. Instead of conservatively backing off of gain and bandwidth, a better model would enable higher performant design.

2. Better noise performance

   Most of the noise in the system did not come from component noise but instead external interference. Noise could be reduced in further iterations by designing a PCB for the active probes with proper shielding of the high impedance traces. The long audio cables used to connect the probes to the amplifier were not shielded. Shielded cables or running the differential signal as a twisted pair would have increased noise performance

3. Increased robustness

   The system was not as robust to the placement of the electrodes as planned. Better modeling would provide data to tune the DRL and magnitudes of the gain stages to increase the robustness of the circuit to use and varying pressure on the user's skin.

5 Conclusion

This project was successful designing and constructing a device to measure EEG/EMG signals. Testing proved to be a major challenge in a project that required a human subject. With only myself as the willing subject, it was difficult to measure my body and analyze and tune a circuit at all the same time. However, despite the lack of a patient subject with no other task to do, the project was effective albeit with shifted goals. The project was made more successful by focusing more on the more compelling demonstration of EMG sensing of blinking rather than the opaque signals of EEG. In both cases, the amplifier presented the same set of challenges and design criterion which were met.